RSC Advances

ROYAL SOCIETY OF CHEMISTRY

www.rsc.org/advances

Synthesis of double gold nanoclusters/graphene oxide and its application as a new fluorescence probe for Hg^{2+} detection with greatly enhanced sensitivity and rapidity

Wu Xiaofei[a], Li Ruiyi[b], Li Zaijun[a,c,*], Liu Junkang[a], Wang Guangli[a] and Gu Zhiguo[a]

[a] *School of Chemical and Material Engineering, Jiangnan University, Wuxi, China*

[b] *The University of Birmingham, Edgbaston, Birmingham, BI5 2TT, United Kingdom*

[c] *Key Laboratory of Food Colloids and Biotechnology, Ministry of Education, Wuxi 214122, China*

We reported synthesis of double gold nanoclusters/graphene oxide (D-GNCs/GO) and its application as new fluorescence probe for detection of Hg^{2+}. The resulting D-GNCs/GO offers greatly improved optical property. The nanosensor based on the hybrid displays surprisingly enhanced sensitivity and rapidity for detection of Hg^{2+}, owing to prominent synergistic effect between GNC@Lys, GNC@BSA and GO.

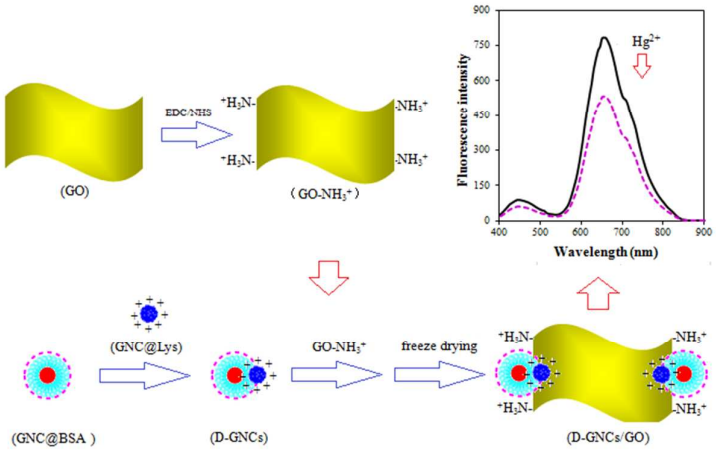

RSC Advances

RSCPublishing

ARTICLE

Synthesis of double gold nanoclusters/graphene oxide and its application as a new fluorescence probe for Hg^{2+} detection with greatly enhanced sensitivity and rapidity

Cite this: DOI: 10.1039/x0xx00000x

Received 00th January 2012,
Accepted 00th January 2012

DOI: 10.1039/x0xx00000x

www.rsc.org/

Wu Xiaofei,[a] Li Ruiyi,[b] Li Zaijun,*[a,c] Liu Junkang,[a] Wang Guangli[a] and Gu Zhiguo[a]

Gold nanoclusters possess outstanding physical and chemical attributes that make them excellent scaffolds for construction of chemical and biological sensors. The paper reported synthesis of double gold nanoclusters/graphene oxide (D-GNCs/GO) and its application as a new fluorescence probe for Hg^{2+} detection. In the study, amine group was introduced into GO sheet through the EDC/NHS mediated reaction to form positively charged GO sheets (GO-NH_3^+). After GNC@Lys was mixed with GNC@BSA to form negatively charged D-GNCs, the D-GNCs was assembled on the surface of GO-NH_3^+ with electrostatic interaction. The study demonstrated that the interaction between GNC@Lys and GNC@BSA increases fluorescence intensity of the GNC@BSA and leads to more sensitive fluorescence response towards Hg^{2+}, which the sensitivity is more than 3-fold that of single GNC@BSA. The interaction between GO and GNCs accelerates the reaction of D-GNCs/GO with Hg^{2+}, which the reaction rate is more than 3-fold that of single D-GNCs. Owing to prominent synergistic effect between GNC@Lys, GNC@BSA and GO, the nanosensor based on the D-GNCs/GO displays an surprisingly enhanced sensitivity and rapidity for Hg^{2+} detection. The fluorescence peak intensity linearly decreases with increasing Hg^{2+} concentration in the range of 1.0×10^{-5}~5.0×10^{-13} M with detection limit of 1.8×10^{-13} M (S/N=3). The analytical method presents an obvious advantage of sensitivity, rapidity and repeatability when compared with present Hg^{2+} optical sensors. It has been successfully applied to detection of Hg^{2+} in water samples. The study also opens a new avenue for fabrication of fluorescent hybrids, which holds great potential applications in sensing, spectral encoding, bioimaging and catalysis.

1 Introduction

Noble metal nanoclusters have many properties that are regulated by their subnanometer dimensions.[1-3] Because of their fascinating features, including the ease of preparation and conjugation, biocompatibility, good water-solubility, excellent stability and large stokes shifts, gold nanoclusters (GNCs) have increasingly received great attention.[4,5] Currently, there are mainly two methods for the synthesis of GNC. One method is based on template-assisted synthesis with polymers[6] or biomolecules as template.[7-9] Another method is relied on monolayer protection in presence of the molecule with thiol ligand.[10] To meet the needs of different applications, some amino acids were also develooped for fabrication of various fluorescent GNCs in the recent years. For example, Ma et al. synthesized an alkanethiol-stabilized GNC based on simply placing histidine, 11-mercaptoundcanoic acid and chloroauric acid together.[11] The resulting GNC provides intense fluorescence, long fluorescence lifetime and considerable stability. More importantly, it also exhibits negligible effect in altering cell proliferation or triggering apoptosis. Qi et al. fabricated a folic acid-functionalized fluorescent GNC for cancer cell imaging.[12] The obtained GNC gives high fluorescence intensity, good photostability and near-infrared fluorescence spectrum. Moreover, several enzymes have also been proven to be excellent scaffolds and reducing agents for synthesis of GNC. Fluorescent properties of the resulting GNCs make them potential labels for biologically motivated studies.[13,14] Although these great grogresses have widened field of GNC application, any one kind of fluorescent GNCs still remains great challenge to simultaneously achieve high sensitivity, rapidity and stability when these were used in chemical and biological sensors.

Recently, the marriage of protein-stabilized GNC with amino acid-stabilized GNC or grapheme oxide (GO) becomes a new hot research. For example, Yang et al. used the marriage of lysine-stabilized GNC (GNC@Lys) with bovine serum albumin-stabilized GNC (GNC@BSA) for detection of Cu^{2+}. The results demonstrated that the marriage will remarkably enhance fluorescence response of the GNC towards Cu^{2+}.[15]

Ren et al. developed a GNC/GO hybrid for cancer cell detection.[16] The study reveals that GO plays an important role in modulating catalytic activity of the supported GNC. Our grpup reported a GNC/GOX/GO as cascade of enzymes for glucose detection. The cascade can offer high fluorescence intensity, largely enhanced catalytic activities towards decomposition of hydrogen peroxide and oxidation of glucose. It was successfully applied to fluorescence detection of glucose in serum samples.[17]

In the study, we focus on the synthesis of double gold nanoclusters/graphene oxide (D-GNCs/GO) and its application as new fluorescence probe for detection of Hg^{2+}. The resulting D-GNCs/GO exhibits strong fluorescence signal, and largely enhanced sensitivity and rapidity towards Hg^{2+}. It was used as a new fluorescence probe for detection of Hg^{2+} in water samples by fluorescence method. The analytical method presents an obvious advantage of sensitivity, rapidity and repeatability when compared with present Hg^{2+} optical sensors.

2 Experimental

2.1 Materials

Hydrogen tetrachloroaurate ($HAuCl_4$), mercury chloride ($HgCl_2$), lysine (Lys), bovine serum albumin (BSA), 1-ethyl-3-(3-dimethylaminopropyl)carbodiimide (EDC), N-hydroxy-succinimide (NHS) and were purchased from Sigma-Aldrich (Mainland, China). Natural flake graphite was obtained from Qingdao Henlide Graphite Company (Qingdao, China) with an average particle size of 20 μm. Phosphate-buffered saline (PBS, pH 7.4, Na_2HPO_4-NaH_2PO_4, 0.05 M) was prepared in the laboratory. GO was synthesized from natural graphite flakes according to modified Hummers method.[18] D-GNCs/GO solution was prepared by dissolving 20 mg of D-GNCs/GO in 20 ml of ultrapure water. Other reagents employed were of analytical regent grade and were purchased from Shanghai Chemical Company (Shanghai, China). Ultrapure water (18.2 MΩ cm) purified from Milli-Q purification system was used throughout the experiment.

2.2 Apparatus

Transmission electron microscope (TEM) analysis was conducted on a JEOL 2010 FEG microscope at 200 keV. The sample was prepared by dispensing a small amount of dry powder in the PBS. Then, one drop of the solution was dropped on 300 mesh copper TEM grids covered with thin amorphous carbon films. EDX mappings were obtained with an FEI Tecnai G2 F30 S-TWIN field emission transmission electron microscope equipped with an EDAX energy-dispersive X-ray spectroscopy operating at 300 kV. Fluorescence spectra were recorded by a Cary Esclipse fluorescence spectrophotometer (Agilent, Japan) with a excitation wavelength of 365 nm. The images were acquired digitally on a Nikon-80i upright fluorescence microscope. Circular dichroism analysis was performed with a MOS-450 circular dichroism spectrometer using a 0.01 cm quartz cell at room temperature. The zeta potential measurements were carried out in a ZETASIZER2000 Zeta Potential Analyzer. PerkinElmer PE 2400 Elemental Analyzer was used for the determination of carbon, oxygen and nitrogen in various graphene materials. SpectrAA 220Z Atomic Absorption Spectrometer was used for gold analysis, in which the sample was digested by aqua regia in advance.

2.3 Synthesis of GNC@BSA

The GNC@BSA was prepared using a reported method.[19] In a typical experiment, all glassware used in the experiments were cleaned in a bath of freshly prepared aquaregia ($HCl:HNO_3$ volume ratio=3:1), and rinsed thoroughly in water. A 50 ml of $HAuCl_4$ solution (20 mM) was added to an equal volume of the BSA solution (50 mg ml^{-1}) under the magnetic stirring. Then, 3.0 ml of the NaOH solution (1.0 M) was introduced and the mixture was allowed to incubate at 37 ℃ for 24 h under vigorous stirring. The color of the solution changed from light yellow to deep brown. The solution was then dialyzed in double distilled water for 48 h to remove unreacted $HAuCl_4$ and NaOH. The obtained GNC solution was stored at 4℃ in refrigerator before use, which the final concentration of gold is 2.2 mM.

2.4 Synthesis of GNC@Lys

GNC@Lys was prepared using the reported method.[15] In a typical synthesis, 20 ml of aqueous $HAuCl_4$ solution (10 mM) was added to 20 ml of aqueous lysine solution (40 mg ml^{-1}). After vigorous stirring for 5 min, 1.5 ml of aqueous NaOH solution (1.0 M) was added into the mixed solution. The mixture was incubated at 37 °C for 12 h. The color of the solution changed from light yellow to deep claret-red. Finally, 4 ml hydrazine was rapidly added to the mixture under vigorous stirring and further incubated at 37 °C for 1 h. The GNC@Lys was purified by triple centrifugation filtration, using Nanosep filters with a molecular weight cut-off of 3 kDa to remove impurities, and then the yellowish GNC@Lys remaining on the filter could be re-suspended readily in water. The obtained GNC@Lys solution was stored at 4℃ in refrigerator before use, which the final concentration of gold is 2.1 mM.

2.5 Synthesis of D-GNCs/GO

To obtain positively charged GO sheets (GO-NH_3^+), 20 mg of graphite oxide was dispersed in 20 ml of the PBS by ultrasonication for 1 h to form homogeneous GO dispersion. Added 1 ml of the mixed EDC/NHS solution (50 mM) to the above dispersion. After 30 min incubation, 0.2 ml of ethylenediamine was added. After another 2 h incubation, the solution was kept overnight at 4℃ and then was dialyzed by the PBS to remove unreacted ethylenediamine. The final concentration of GO is obout 0.5 mg ml^{-1}. Next, the

GNC@BSA (4 ml) was mixed with the GNC@Lys (0.24 ml). After incubation under vigorous shaking at room temperature, 0.5 ml of the GO-NH_3^+ was added into the mixted solution. The solution was vigorously shaked for 1h. Finally, the mixed solution was dried by freeze drying to obtain solid D-GNCs/GO. The product was stored at 4 ℃ for further use.

2.6 Detection of Hg^{2+}

The Hg^{2+} solution of known concentration or real water sample was mixed with 1 ml of the D-GNCs/GO solution. After 5 min incubation, the solution was subjected to fluorescence measurements on the fluorescence spectrophotometer with an excitation wavelength of 365 nm.

3 Results and discussion

3.1 Synthesis of D-GNCs/GO

Synthesis of D-GNCs/GO includes four assemble processes, i.e. the preparations of GO-NH_3^+, D-GNCs and D-GNCs/GO and freeze drying of D-GNCs/GO (shown in **Fig.1**). First, graphite oxide was well dispersed in ultrapure water by ultrasonication to form homogeneous GO dispersion. Then, amine group was introduced on the surface of GO sheet through the EDC/NHS mediated reaction between carboxylic acid and ethylenediamine to produce GO-NH_3^+. Zeta potential of the resulted GO-NH_3^+ is +62.7±0.62 mV, indicating strong positive charge. Next, GNC@BSA was mixed with the amounts of GNC@Lys. Because zeta potentials of the GNC@BSA and GNC@Lys are -32.8±0.52 mV, verifying strong negative charge, and +26.10±0.16 mV, verifying strong positive charge, the above mixing will lead to form D-GNCs hybrid due to their electrostatic attraction. Moreover, the process was also confirmed by observing change of fluorescence under ultraviolet radiation using a WFH-203 ultraviolet analyzer (shown in **Fig.2**). In strong drive of the electrostatic attraction, the GNC@BSA with red fluorescence will rapidly close to GNC@Lys with blue fluorescence. The process can complete within 2 min. In the reaction, the amounts of GNC@Lys was significantly less than the amount of GNC@BSA, thus formed D-GNCs shows red fluorescence and its zeta potential is about -20.2±0.37 mV, verifying strong negative charge. Next, the D-GNCs was assembled on the surface of GO-NH_3^+ to form stable D-GNCs/GO hybrid due to their electrostatic attraction. Moreover, we also observed a considerable decrease in zeta potential of the GO-NH_3^+ after addition of D-GNCs. This confirms again the formation of D-GNCs/GO through electrostatic adsorption. Finally, the hybrid was dried by freeze drying to enhance long-term stability.

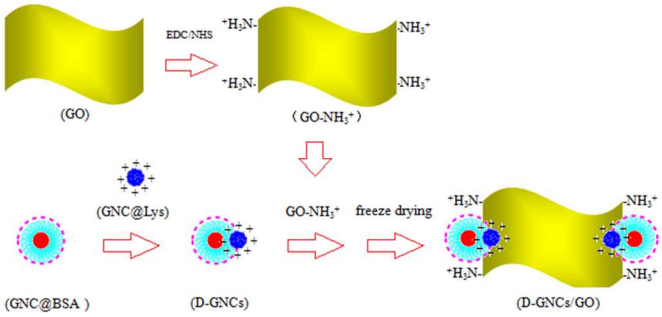

Fig.1 The procedure for synthesis of D-GNCs/GO

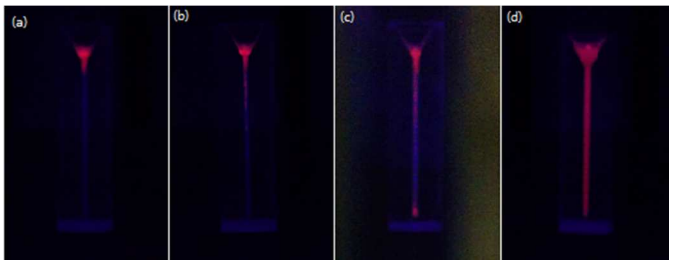

Fig.2 Fluorescence images of GNC@Lys (blue fluorescence) after added GNC@BSA (red fluorescence) at 0.1 min (a), 1 min (b), 1.5 min (c) and 2 min (d)

3.2 Structure characterization

The as-prepared D-GNCs/GO was characterized by TEM, enlarged TEM, EDX and XPS and their results were shown in **Fig.3**. TEM analysis shows that D-GNCs/GO contains many wrinkled GO sheets, and GNCs were well dispersed on the surface of GO sheets. The enlarged TEM shows that average diameter of the GNCs is about 3-4 nm with a narrow particle size distribution. Further, EDX analysis reveals that Au cores in D-GNCs are about 1-2 nm and no Au core in pairs could be observed. The result demonstrates that the GNC@Lys don't enter into inside of the GNC@BSA and is located at the surface of GNC@BSA. Owing to blocking of BSA shell, the

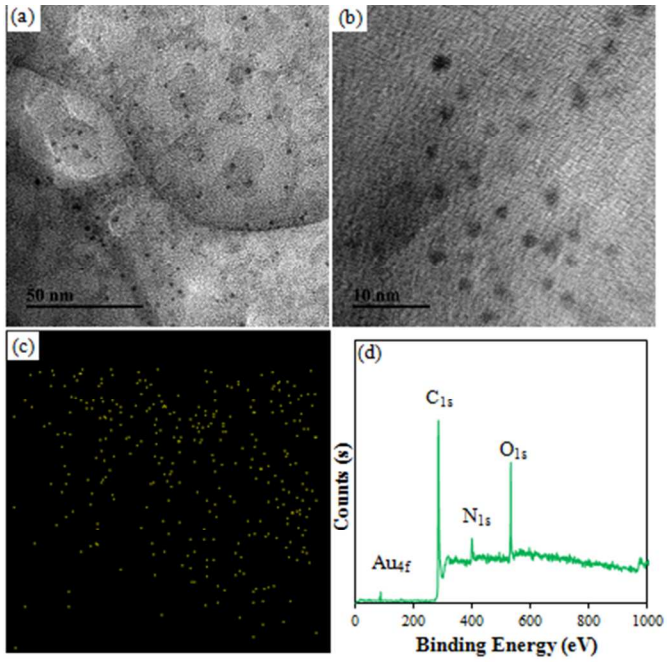

Fig.3 TEM (a), enlarged TEM (b), EDX (Au_{4f}) (c) and XPS patterns (d) of D-GNCs/GO

combination of GNC@Lys with GNC@BSA cann't form real Au core in pairs. XPS technology is powerful tool for studying on the surface chemical properties of materials. On the XPS spectrum of the D-GNCs/GO there are five peaks at 83.5, 87.3, 284.4, 399.6 and 531.9 eV. The peaks at 284.4, 399.6 and 531.9 eV could be assigned to C_{1s}, N_{1s}, and O_{1s}, which come from BSA, GO and Lys. The peaks at 83.5 and 87.3 eV could be assigned to Au_{4f}, verifying the success of GNCs modification on the surface of GO sheets. Moreover, gold content in the D-GNCs/GO was determined by atomic absorption spectrometry. The result is about to 3.88 wt% gold in the hybrid.

3.3 Optical property

D-GNCs/GO is composed of two kinds of GNCs and GO. Thus, the interaction between them may seriously affect on the optical properties. **Fig.4** presents fluorescence spectra of single GNC@Lys, single GNC@BSA and D-GNCs. It can be seen that GNC@Lys only has one fluorescence emission peak at 440 nm. GNC@BSA offers two fluorescence emission peaks, in which the peak at 440 nm is obviously weaker than the peak at 660 nm. Different from sing GNC, fluorescence spectrum of the D-GNCs exists two strong fluorescence emission peaks. One peak lies at 440 nm which results from the GNC@Lys. Another peak lies at 660 nm which results from the GNC@BSA. The fact demonstrates that the combination of GNC@Lys with GNC@BSA does not change the location and shape of fluoresence emission peak of GNC. This should be attributed that GNC@BSA exists a relatively thick BSA shell (3-4 nm) arounding gold core. The shell effectively prevents the energy transfer between GNC@BSA and GNC@Lys, thus the each GNC in the hybrid can keep its original optical characteristic. Moreover, the characteristic was also demonstrated by analysis result of fluorescence microscopy

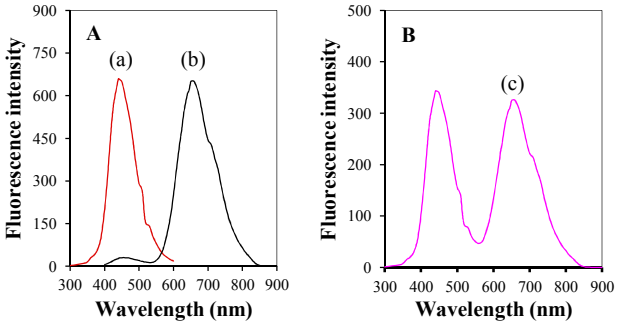

Fig.4 Fluorescence spectra of single GNC@Lys and single GNC@BSA (A), and D-GNCs (B)

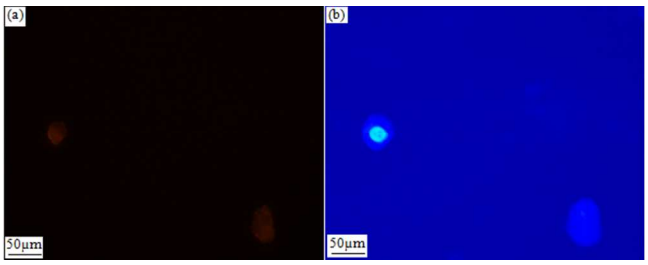

Fig.5 Photomicrographs of D-GNCs. The blue emission of 435-480 nm from GNC@Lys (a) was obtained by using the excitation wavelength of 340-380 nm. The red emission of 550-605 nm from GNC@BSA (b) was obtained by using the excitation of 250-540 nm.

imaging (shown in **Fig.5**). The property of D-GNCs/GO is very important to overcome spectral interference from the energy transfer between different components, the hybridization of protein-stabilized GNC with amino acid-stabilized GNC can be easily used for fabrication of various multicolor fluorescent microspheres for multi-component analysis and biochip.

To investigate effect of the interaction between GNC@Lys and GNC@BSA on the fluorescence intensity, the fluorescence spectrum of GNC@BSA before and after added GNC@Lys was measured. **Fig.6**A shows that the addition of GNC@Lys will result in an increase of the fluorescence intensity when compared with single GNC@BSA. Because the change value at 440 nm is the same as fluorescence intensity of the GNC@Lys added. The fact reveals that the interaction between GNC@Lys and GNC@BSA does not influence on the fluorescence intensity of GNC@Lys. However, the fluorescence intensity of GNC@Lys at 660 nm is close to zero, the change at 660 nm demonstrates that the interaction between GNC@Lys and GNC@BSA can increase the fluorescence intensity of GNC@BSA. Further, we examined the effect of GNC@Lys content on the fluorescence intensity of GNC@BSA. Fig.6B indicates that the fluorescence intensity of GNC@BSA will increase with the increase of GNC@Lys content when GNC@Lys is less than 6%. The fluorescence intensity at 660 nm reaches the maximum value when GNC@Lys is up to 6%. After that, the fluorescence intensity will rapidly decrease with the increase of GNC@Lys content. The above change at 660 nm should be attributed to two factors. The first factor is that amino groups attached on the surface of GNC@Lys combines with carbonxyl group or hydroxyl group attached on the surface of GNC@BSA due to their electrostatic attraction. The combination enhances the structure stability of BSA on the surface of GNC@BSA,

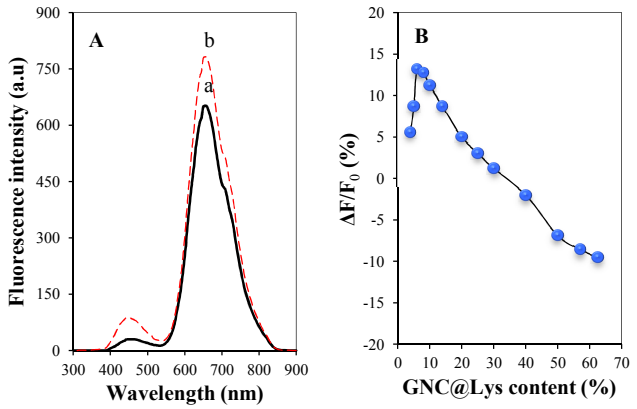

Fig.6 Fluorescence spectra of the GNC@BSA before (a) and after (b) added 6% GNC@Lys (A) and relationship cure of change ratio ($\Delta F/F_0$) in fluorescence peak intensity of D-GNCs at 660 nm with GNC@Lys content (B)

which will result in an increase in the fluorescence intensity of GNC@BSA.[20] The second factor is that the interaction between two opposite electric fields produced from two kinds of GNCs produces strong withdrawing electron effect of GNC@BSA, which will lead to decrease the fluorescence intensity of GNC@BSA. To improve BSA stability only needs a small amounts of GNC@Lys, and the withdrawing electron effect will rapidly increase with the increase of GNC@Lys. Therefore, a relatively low concentration of GNC@Lys will result in the increase of the fluorescence intensity of GNC@BSA, and a relatively hgih concentration of GNC@Lys will result in the decrease of fluorescence intensity of the GNC@BSA.

D-GNCs/GO can act as new fluorescence probe for detection of various metal ions. **Fig.7** presents the fluorescence spectra of GNC@BSA and D-GNCs/GO before and after added 1×10^{-12} M. It can be seen that the D-GNCs/GO gives a more sensitive fluorescence response towards Hg^{2+}, which the sensitivity is more than 3-fold that of single GNC@BSA. To understand the reaction mechanism, D-GNCs/GO before and

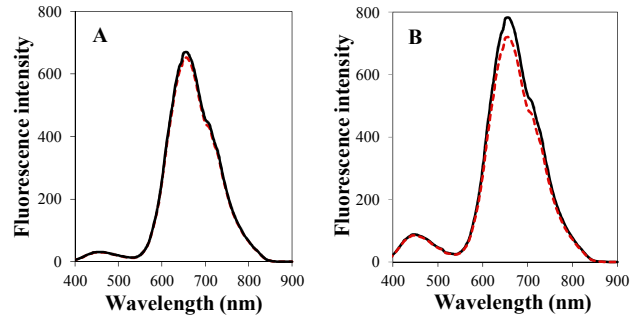

Fig.7 Fluorescence spectra of GNC@BSA (A) and D-GNCs/GO (B) before (upper) and after (down) added Hg^{2+} (1×10^{-12} M)

after reacted with Hg^{2+} was characterized by TEM analysis. **Fig.8** shows that the reaction results in an obvious agglomeration of GNCs. On the one hand, Hg^{2+} reacts with mercapto group attached on the surface of GNC@BSA to form Hg-S covalent bond, which will destroy Au-S bond and result in the agglomeration of GNCs.[21] On the other hand, Hg^{2+} reacts with amino groups attached on the surface of GNC@Lys to form Hg-N coordinate bond, which will result in

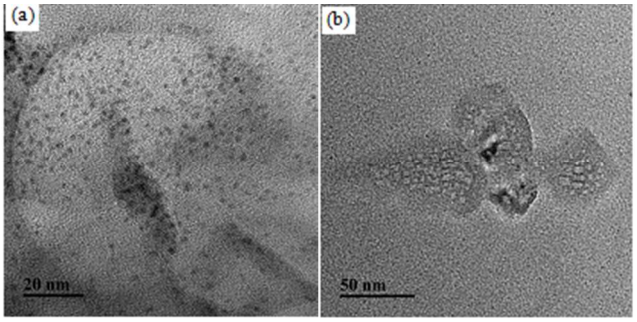

Fig.8 TEM images of D-GNCs/GO before (a) and after (b) added Hg^{2+}

the agglomeration of GNCs. The interaction result of the above two factors will lead to greater degree of GNC agglomeration and more sensitive fluorescence response when compared with single GNC@BSA.

The interaction of GO with D-GNCs was examined by studying on kinetic performance of the reaction between D-GNCs and Hg^{2+}. **Fig.9** shows that fluorescence peak intensity of the D-GNCs/GO will rapidly decrease with the increase of the reaction time. When the time exceeds 4 min, the fluorescence intensity reaches its minimum value. The result confirms that the reaction can complete with 4 min, which the rate is hgiher than 3-fold that of single D-GNCs. At the same time, the fact also reveals that the introduction of GO will remarkably accelerate the reaction of D-GNCs with Hg^{2+}. To understand the effects of GO, circular dichroism technique was used for studying on the structure change of BSA on the surface of GNC before and after the addition of GO. Then, the ratio of each secondary structure in the BSA was calculated

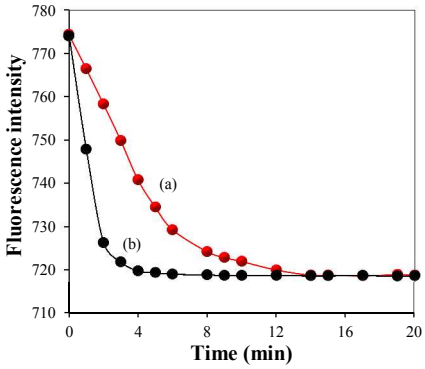

Fig.9 Changes of the fluorescence peak intensity of D-GNCs (a) and D-GNCs/GO (b) added Hg^{2+}

from the circular dichroism spectrum. We can draw two conclusions from **Fig.10**. The one conclusion is that the introduction of GNC@Lys does not change secondary

structures of BSA on the surface of GNC@BSA. The another conclusion is that the use of GO will result in an obvious

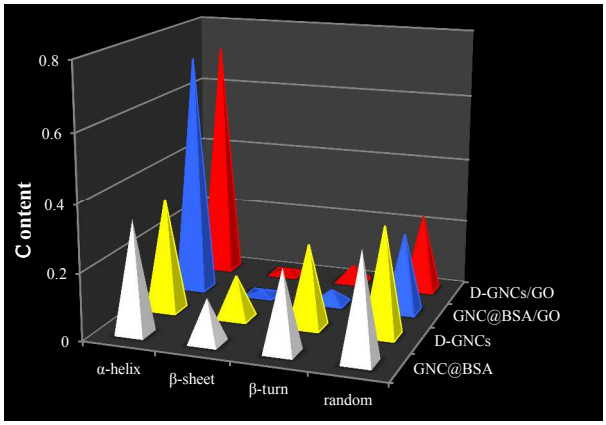

Fig.10 Secondary structures of the hybrids containing GNC@BSA

increase of the α-helix, and decrease of the β-sheet and random compared with single GNC@BSA. The change in secondary structure will remarkably increase the exposure degree of gold atoms in the GNC, the interactions between GO sheet and GNC makes gold atom can fully contact with Hg^{2+}, which will remarkably improve response sensitivity towards Hg^{2+}.

Solvation dynamics of D-GNCs/GO was studied by measuring the fluorescence spectra with different excitation wavelength. **Fig.11** shows that the peak fluorescence emission around 440 nm will obviously change with the excitation wavelength changes. Although the fluorescence of GO depends the excitation wavelength,[22] its fluorescence intensity is very weak. Thus, the above peak fluorescence emission change mainly comes from GNC@Lys. We suggest that strong excitation wavelength dependent fluorescence in GNC@Lys is originated from the "giant red-edge effect", which breaks Kasha's rule. When GNC@Lys is present in a polar solvent, the solvation dynamics slow down to the same time scale as the fluorescence due to local environment of the GNC@Lys. The giant red-edge effect of GNC@Lys disappears in a nonpolar solvent, leading to narrow fluorescence peak that is independent of the excitation wavelength. Discovery of the underlying strong excitation wavelength dependent fluorescence mechanism provides guidelines for the design of GO and GNC-based optical devices. In contrast, the peak fluorescence emission around 660 nm does not change with the excitation wavelength changes, indicating that the peak photoluminescence of GNC@BSA is independent of the wavelength of the excitation source. This is because the BSA shell on the surface of GNC@BSA will gold core and external solvent completely isolated. The excited electrons relax to the band edge before fluorescence begins regardless of their initial excitation energy. The peak fluorescence wavelength of GNC@BSA is the same as long as the electrons are excited within the same band.

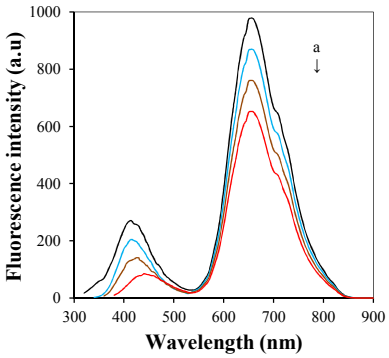

Fig.11 Fluorescence spectra of D-GNCs/GO (A) and GNC@Lys (B) with the excitation wavelength of 300 nm, 320 nm, 340 nm and 360 nm (from a to d)

3.4 Analytical characteristics

The nanosensor based on the D-GNCs/GO was used for Hg^{2+} detection. **Fig.12** displays fluorescence response of the nanosensor in different concentration of Hg^{2+} and calibration plot of logarithmic Hg^{2+} concentration vs. corresponding maximum fluorescence intensity. The fluorescence intensity will rapidly decrease with the increase of Hg^{2+} concentration. When Hg^{2+} concentration is in the range from 1.0×10^{-5} to 5.0×10^{-13} M, the fluoresence intensity linearly decreases with the increase of Hg^{2+} concentration. The linear equation was F=-19.67C+494.42, with statistically significant correlation coefficient of 0.9974, which F is the fluorescence intensity at 660 nm and C is logarithmic Hg^{2+} concentration. The detection limit was found to be 1.8×10^{-13} M that was obtained from the signal-to-noise characteristics of these data (S/N=3), which is better than other optical sensors for detection of Hg^{2+} such as Lys VI-GNC (3×10^{-12} M),[23] GNC@BSA (8×10^{-8} M) [24] and graphene quantum dots (1.2×10^{-8} M).[25]

The nanosensor was repeatedly measured ten times in a 5.0×10^{-6} M of Hg^{2+} standard solution under the same conditions. A relative standard deviation of 2.1% for the measurements was obtained, indicating good precision. The D-GNCs/GO product was stored in at 4¤ and its sensitivity for detection of Hg^{2+} was checked every week. The fluorescence intensity remains the initial response of 99.7% at least after the period of eighteen weeks, indicating an excellent long-term stability.

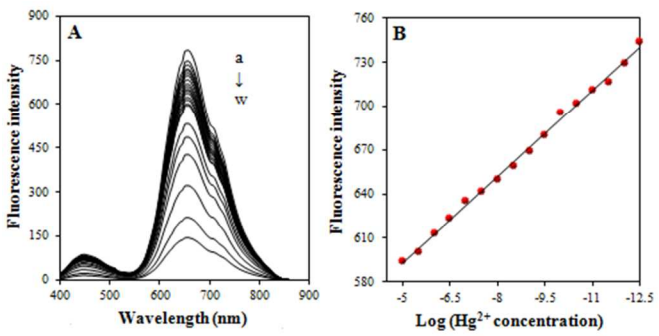

Fig.12A: Fluorescence response of D-GNCs/GO in 0.0, 5×10^{-13}, 1×10^{-12}, 5×10^{-12}, 1×10^{-11}, 5×10^{-11}, 1×10^{-10}, 5×10^{-10}, 1×10^{-9}, 5×10^{-9}, 1×10^{-8}, 5×10^{-8}, 1×10^{-7}, 5×10^{-7}, 1×10^{-6}, 5×10^{-6}, 1×10^{-5}, 5×10^{-5}, 1×10^{-4}, 5×10^{-4}, 1×10^{-3}, 5×10^{-3} and 1×10^{-2} M of Hg^{2+} (from a to w). B: Calibration plots of concentration of logarithmic Hg^{2+} vs. fluorescence intensity at 660 nm

To test selectivity of the proposed method, the effect of various metal ions on the fluorescence of D-GNCs/GO was investigated, including Li^+, Na^+, K^+, Ca^{2+}, Mg^{2+}, Ba^{2+}, Cu^{2+}, Fe^{3+}, Co^{2+}, Ni^{2+}, Al^{3+}, Ag^+, Zn^{2+}, Pb^{2+}, Mn^{2+} and Sr^{2+}. Among these ions, Li^+, Na^+, K^+, Al^{3+}, Ca^{2+}, Mg^{2+}, Ba^{2+}, Zn^{2+}, Pb^{2+}, Mn^{2+} and Sr^{2+} don't react with D-GNCs/GO to create an obvious agglomeration of GNCs, an addition of 0.2 M for the each ion produces a less than 5% decrease in the fluorescence signal. Co^{2+} and Ni^{2+} can combine with amino groups attached on the surface of GNC@Lys to form stable coordination bond, an addition of 0.05 M Co^{2+} or Ni^{2+} will result in relatively big decrease in the intensity (about 25%). Cu^{2+} can react with amino groups attached on the surface of GNC@Lys to form stable coordination bond, and mercapto groups attached on the surface of GNC@BSA to form Cu-S covalent bond. The interaction result of the above two factors will lead to a greater degree of GNC agglomeration and bigger derease in the fluorescence singal compared with Ni^{2+} and Co^{2+}. An addition of 1×10^{-2} M Cu^{2+} results in 92% derease in the intensity. However, these effects may be easily elimated by EDTA. The study shows that the use of 1.5×10^{-3} M EDTA as masking agent can well overcome the interference from Cu^{2+}, Ni^{2+} and Co^{2+} for detection of Hg^{2+}.

3.5 Determination of trace Hg^{2+} in water samples

The feasibility of the newly developed method for possible applications was investigated by analyzing real water samples. All water samples including lake water, river water, well water and rain water were collected from Jiangsu province in China. The spike and recovery experiments were performed by measuring the fluorescence responses to the sample in which the known concentrations of Hg^{2+} was added. The concentration of Hg^{2+} in water sample was determined from the calibration curve and the value was used to calculate the concentration in the original sample. The mean ± SD of each sample and recovery of each spiked sample were calculated, and the values are reported in **Table 1**. The recovery of Hg^{2+} for spiked samples analysis is in the range of 95.2-105.4%. There is a very good agreement between the results obtained by proposed method and cold vapor generation atomic absorption spectrometry (CVGAAS).[26] These indicated proposed method has a good accuracy and precision.

Table 1 Determination of Hg^{2+} in water sample (N=5)[a]

Samples	Hg^{2+} found by proposed method (nM)	Hg^{2+} found by CVGAAS (nM)	**Recovery (%)**
Lake water	0.37±0.10 F=1.44, t=0.58	0.39±0.12	99.6
River water	1.21±0.14 F=1.61, t=0.18	1.20±0.11	95.2
Well water	2.06±0.17 F=1.37, t=0.57	2.11±0.20	101.4
Rain water	0.12±0.06 F=1.2, t=0.33	0.11±0.09	105.4

[a] Results expressed as: $\mathbf{X \pm \frac{st}{\sqrt{n}}(n = 5)}$, where X is the mean of n observations of x, s is the standard deviation, t is distribution value chosen for the desired confidence level, the t- and F-values refer to comparison of the proposed method with the hexokinase method. Theoretical values at 95% confidence limits: F = 6.39, t = 2.78

4 Conclusions

D-GNCs/GO has been successfully synthesized and applied for detection of Hg^{2+}. The study for the first find that the interaction of GNC@BSA with GNC@Lys can increase the fluorescence intensity of the GNC@BSA and the sensitivity of fluorescence response towards Hg^{2+}. The interaction of GO with GNC@BSA can increase exposure degree of the active site and result in largely enhanced the reaction rate of D-GNCs/GO with Hg^{2+}. Owing to synergistic effect between GNC@Lys, GNC@BSA and GO, the nanosensor based on the D-GNCs/GO exhibits excellent long-term stability, sensitivity, repeatability and stability. More importantly, the study opens a new avenue for the fabrication of various fluorescent hybrids, which holds great potential applications in sensing, spectral encoding, bioimaging and catalysis.

Acknowledgements

The authors acknowledge the financial support from the National Natural Science Foundation of China (No.21176101), the Fundamental Research Funds for the Central Universities (No.JUSRP51314B), MOE & SAFEA for the 111 Project (B13025) and the country "12th Five-Year Plan" to support science and technology project (No. 2012BAK08B01).

Notes and references

[a] *School of Chemical and Material Engineering, Jiangnan University, Wuxi, China. Fax:86051085811863; Tel:13912371144; e-mail: zaijunli@263.net*
[b] *The University of Birmingham, Edgbaston, Birmingham, BI5 2TT, United Kingdom*
[c] *Key Laboratory of Food Colloids and Biotechnology, Ministry of Education, Wuxi 214122, China*

1 L.A. Peyser, A.E. Vinson, A.P. Bartko and R.M. Dickson, *Science*, 2001, **291**, 103.
2 A.A. Herzing, C.J. Kiely, A.F. Carley, P. Landon and G.J. Hutchings, *Science*, 2008, **321**, 1331.
3 Z.Y. Li, N.P. Young, M. Di Vece, S. Palomba, R.E. Palmer, A.L. Bleloch, B.C. Curley, R.L. Johnston, J. Jiang and J. Yuan, *Nature*, 2008, **451**, 46.
4 I. Diez and R. H. A. Ras, *Nanoscale*, 2011, **3**, 1963.

5 H. C. Yeh, J. Sharma, J. J. Han, J. S. Martinez and J. H. Werner, *Nano Lett*., 2010, **10**, 3106.
6 J. Zheng, C.W. Zhang and R.M. Dickson, *Phys. Rev. Lett*., 2004, **93**, 077402.1.
7 J. P. Xie, Y. G. Zheng and J. Y. Ying, *J. Am. Chem. Soc.*, 2009, **131**, 888.
8 C. L. Liu, H. T. Wu, Y. H. Hsiao, C. W. Lai, C. W. Shih, Y. K. Peng, K. C. Tang, H. W. Chang, Y. C. Chien, J. K. Hsiao, J. T. Cheng and P. T. Chou, *Angew. Chem., Int. Ed.*, 2011, **50**, 7056.
9 T. A. C. Kennedy, J. L. MacLean and J. W. Liu, *Chem. Commun*., 2012, **48**, 6845.
10 M. Zhu, C. M. Aikens, F. J. Hollander, G. C. Schatz and R. Jin, *J. Am. Chem. Soc.*, 2008, **130**, 5883.
11 P.P. Bian, J. Zhou, Y.Y. Liu and Z.F. Ma, *Nanoscale*, 2013, **5**, 6161.
12 J. Qiao, X.Y. Mu, L. Qi, J.J. Deng and L.Q. Mao, *Chem. Commun*., 2013, **49**, 8030.
13 H. Kawasaki, K. Yoshimura, K. Hamaguchi and R. Arakawa, *Anal. Sci.*, 2011, **27**,591.
14 Y. Chen, Y. Wang, C.X. Wang, W.Y. Li, H.P. Zhou, H.P. Jiao, Q. Lin, C. Yu, *J. Colloid Interface Sci.*, 2013, **396**, 63.
15 X.M. Yang, L. Yang, Y. Dou and S.S. Zhu, *J. Mater. Chem. C*, 2013, **1**, 6748.
16 Y. Tao , Y.H. Lin , Z.Z. Huang , J.S. Ren and X.G. Qu, *Adv. Mater.*, 2013, **25**, 2594.
17. X.F. Wu, R.Y. Li and Z.J. Li, *RSC Adv.*, 2014, 4, 9935.
18 L. Yan, H. Kong and Z.J. Li, *Acta Chimica Sinica*, 2013, **71**, 822.
19 H. Lin, L.J. Li, C.Y. Lei, X.H. Xu, Z. Nie, M.L. Guo, Y. Huang and S.Z.Yao, *Biosens. Bioelectron.*, 2013, **41**, 256.
20 M. Zhang, Y.Q. Dang, T.Y. Liu, H.W. Li, Y.Q. Wu, Q. Li, K. Wang, and B. Zou, *J. Phys. Chem. C*, 2013, **117**, 639.
21 K.S. Park, M.I. Kim, M.A. Woo, H.G. Park, *Biosensors and Bioelectronics*, 2013, **45**, 65.
22 S.K. Cushing, M. Li, F.Q. Huang, and N.Q. Wu, *ACS Nano*, 2014, **8** ,1002.
23 Y.H. Lin and W.L. Tseng, *Anal. Chem.*, 2010, **82**, 9194.
24 D.H. Hu, Z.H. Sheng, P. Gong, P.F. Zhang and L.T. Cai, *Analyst*, 2010, **135**, 1411.
25 L.L. Li, G.H. Wu, T. Hong, Z.Y. Yin, D. Sun, E.S. Abdel-Halim, J.J. Zhu, *ACS Appl. Mater. Interfaces*, 2014, **6**, 2858.
26 M.T. Peng, Z.A. Li, X.D. Hou, C.B. Zheng, *J. Anal. At. Spectrom*., 2014, **29**, 367.

